

# RSC Advances



This is an *Accepted Manuscript*, which has been through the Royal Society of Chemistry peer review process and has been accepted for publication.

*Accepted Manuscripts* are published online shortly after acceptance, before technical editing, formatting and proof reading. Using this free service, authors can make their results available to the community, in citable form, before we publish the edited article. This *Accepted Manuscript* will be replaced by the edited, formatted and paginated article as soon as this is available.

You can find more information about *Accepted Manuscripts* in the [Information for Authors](#).

Please note that technical editing may introduce minor changes to the text and/or graphics, which may alter content. The journal's standard [Terms & Conditions](#) and the [Ethical guidelines](#) still apply. In no event shall the Royal Society of Chemistry be held responsible for any errors or omissions in this *Accepted Manuscript* or any consequences arising from the use of any information it contains.

# The influence of hygrothermal ageing on mechanical properties and thermal degradation kinetics of long glass fibre reinforced polyamide 6 composites filled with sepiolite

Weidi He<sup>1</sup>, Nian Liu<sup>1</sup>, Xiaolang Chen<sup>1,3,\*</sup>, Jianbing Guo<sup>2,\*</sup>, Tao Wei<sup>2</sup>

(1.Key Laboratory of Advanced Materials Technology Ministry of Education, School of Materials Science and Engineering, Southwest Jiaotong University, Chengdu 610031, China; 2.National Engineering Research Center for Compounding and Modification of Polymer Materials, Guiyang 550014, China; 3. The State Key Laboratory of Polymer Materials Engineering, Polymer Research Institute of Sichuan University, Chengdu 610065, China)

**Abstract:** In this article, the influence of relatively long time hygrothermal ageing on long glass fibre reinforced polyamide 6 (LGF/PA6) composites filled with sepiolite (Sep) are analyzed. The composites with different weight fraction of Sep are exposed in hygrothermal environment of 80°C and RH 95% for 0–20 days. The mechanical properties with different ageing time show a decrease in tensile strength and an increase in impact strength. The scanning electronic microscope (SEM) photos of the impact fracture indicate that a better adhesion of the interface between glass fibre and polymer matrix in the composites filled with Sep after ageing process. Then the thermal stability and degradation kinetics of the composites with different filler fraction and ageing time are studied by thermal gravimetric analysis (TGA) with the methods of Kissinger, Friedman and Flynn-Wall-Ozawa in dynamic measurements. Calculated apparent activation energy ( $E$ ) by the three methods shows that the composites without Sep have an obviously decrease in the value of  $E$  after ageing, however, the  $E$  values of the composites filled with Sep have a slight increase.

**Key words:** Long glass fibre reinforced polyamide 6; Sepiolite; Hygrothermal ageing; Thermal degradation kinetics.

---

\* Corresponding author. E-mail address: [chenxl612@sina.com](mailto:chenxl612@sina.com) (X. L Chen); [guojianbing\\_1015@126.com](mailto:guojianbing_1015@126.com) (J. B Guo)

## 1. Introduction

In the recent years, long glass fibre (LGF) reinforced thermoplastic polymer composites have been widely used in semi-structure and engineering applications [1–3]. Especially LGF reinforced polyamide 6 (PA6/LGF) composites have an excellent heat resistance, corrosion resistance and mechanical properties. Nowadays, thermoplastic composites are more and more used in applications in which they are exposed to severe hygrothermal environments combining high temperature and moisture. In this kind of environment, water absorption induces a severe decrease of the mechanical properties of the composites that are not only related to plasticisation and hydrolysis, modification of the polymer matrix but also to debonding affecting the fibre-matrix interface [4, 5].

Sepiolite (Sep) is a family of fibrous hydrated magnesium silicate with the theoretical half unit-cell formula  $\text{Si}_{12}\text{O}_{30}\text{Mg}_8(\text{OH})_4(\text{OH}_2)_4 \cdot 8\text{H}_2\text{O}$ , similar to the 2:1 layered structure of montmorillonite, consisting of two tetrahedral silica sheets enclosing a central sheet of octahedral magnesia [6–8]. These layers create a unique paralleled tunnels structure which has a high specific surface area and pore volume to accommodate exchangeable ions, radicals and water molecules and provide an ion exchange ability and water absorption capacity [9]. Because of the hollow structure and the excellent absorption capacities, Sep has some advantages of low weight, high intensity and low price to be widely used in polymer matrix composites [10]. In recently, some progress has been achieved in the organic modification of Sep by surfactant and coupling agent grafting [11–13].

It has been well established that the properties of engineer plastics are affected in different environment factors. However, there is lack of information on the LGF reinforced PA6 composites for serving in hygrothermal environment, especially with regard to the thermal degradation kinetics after ageing. In this work, mechanical

properties of LGF reinforced PA6 composites filled with Sep are evaluated both by differing weight content of Sep and different hygrothermal ageing time. The thermal stability and degradation kinetics of the unaged and aged composites with different contents of Sep, as well as the apparent activation energy of the process, are analyzed by three typical methods. The aim of this work is to evaluate the protection effect of Sep filled in PA6/LGF composites and find out the feasibility of using Sep to fill LGF reinforced PA6 composites in hygrothermal environment by thermal kinetic analysis methods.

## 2. Experimental

### 2.1. Materials

The polyamide 6 (PA6) resins, a standard viscosity grade product, were produced by Yueyang Petrochemic Co., Ltd., China. The long glass fibre (LGF) with the diameter 17  $\mu\text{m}$  was obtained from Chongqing Polycomp International Corporation, China. And the surface of LGF was treated by silane coupling agent. The continuous glass fibre rovings used were of grade ECT4301. Sepiolite (Sep) was purchased from Jinjianshi Petrochemic Co., Ltd., Shijiazhuang, China.

### 2.2. Preparation of samples

The Sep powders were acidized by hydrochloric acid of 1 mol/L for 4 h at 80°C; Then the acidized Sep powders were suction filtrated and treated by KH550 silane coupling agent.

PA6/Sep masterbatches were prepared by mixing different fraction of Sep and PA6 of using a two-screw extruder (TSE-40A, L/D=40, D=40 mm, Coperion Keya machinery, Co., Ltd., China) at the temperatures of 200–250 °C. The PA6 was dried for 4 hours at 90°C to remove moisture water before use. The PA6/LGF composites were blended in the same two-screw extruder and fibres were kept at the fraction of

50 wt%. The continuous strand was then cut into pellets with the length of 11 mm for injection molding.

PA6/LGF extrudates were dried at 90°C for 4 hours, and then were blended with the PA6/Sep masterbatches (at the mass ratio to make the content of glass fibre staying at 30 wt% in the composites). Blended composites were injection molded at 220–265°C into standard specimens for testing and characterization. PA6/LGF/Sep composites were put into a hygroyhermal testing chamber which keeps the temperature at 80°C and relative humidity of 95%. The hygothermal ageing lasts 20 days, and each 5 days several specimens were taken out for testing.

### *2.3. Measurements and characterization*

#### *2.3.1. Mechanical properties*

The tensile strength were measured by the Material Testing Machine typed WDW-10C (Shanghai Hualong Test Instrument co., Ltd., China), with the tensile speed of 50mm/min. The impact strength was measured by the LCD type plastic pendulum impact testing machine ZBC-4B (Shenzhen Xinsansi Measurement Technology co., Ltd., China). All mechanical tests were performed at the room temperature of  $25 \pm 2^\circ\text{C}$

#### *2.3.2. Scanning electronic microscopy (SEM)*

The SEM images obtained on a KYKY-2800B (KYKY Technology Development Co. Ltd., China.) were used to investigate the fracture surface after impact testing of some typical samples. SEM graphs of the composites were recorded after gold coating surface treating, with the accelerating voltage of 25 kV.

#### *2.3.4. Thermaogravimetric analysis (TGA)*

The thermal degradation of composites were investigated by a thermogravimetric analyzer (Q-50 instruments, TA Co., Ltd., USA) under 60 ml/min of balanced gas and

40 ml/min of sample gas flow of high purity grade nitrogen, respectively. About 5–10 mg of each sample was put in a platinum pan and heat from room temperature to 700 °C at the heating rates of 10, 20, 30, and 40 °C/min under N<sub>2</sub> atmosphere.

### 3. Results and discussion

#### 3.1. Mechanical properties

Fig.1 shows the variations of tensile strength with different ageing time. In the early period (first 5 days) of ageing period, all the samples have an obvious decrease in tensile strength in the severe ageing condition of the hygrothermal condition, which is mainly attributed to the PA6 matrix molecular chain break and glass fibre interface failure caused by the temperature and water molecule diffusion. With increasing hygrothermal ageing time, the tensile strength of both samples of PA6/LGF and PA6/LGF/Sep stay at a relatively stable level. It's interesting that when the samples are taken out of the oven after long time ageing, there are some wet sepiolite powders attached on PA6/LGF/Sep samples, some powders even drop out of samples. Unfortunately, after the attached powders drop in moving course, it's difficult to distinguish them from unaged ones. This can be attributed to the migration of sepiolite from inner structure to sample surface. With further prolonging ageing time, the sepiolite particles gather on the surface by the absorbed water flow inside the composites, which causes a decrease of water diffusion in the composites in hygrothermal environment.

The variations of impact strength of PA6/LGF/Sep with different contents of sepiolite are displayed in Fig. 2. In the first 5 days of ageing, it is clearly observed that the impact strength of all the samples increases significantly, and then have a slight decrease with increasing ageing time, however, the values of impact strength still stay at a much higher level than unaged ones. Because of the water absorption of PA6, it

can be attributed to the effect of physical water plasticization caused by the diffused water in PA6 matrix. The decrease of tensile strength and increase of impact strength show that the material has become ductile.

More clearly, to analysis the effect of sepiolite on the mechanical properties of PA6/LGF composites in hygrothermal ageing procedure, the retention rate of tensile and impact strength of PA6/LGF composites with various sepiolites contents in different ageing time is calculated and exhibited in Figs. 3 and 4, respectively. The addition of Sep has a very large effect on the retention rate of tensile and impact strength. It can be clearly found from Fig. 3 that the retention rate of tensile strength of PA6/LGF sample after 10 days ageing can be recognized to a boundary. The sample with 6% wt Sep has a higher retention rate of more than 80% in tensile strength while that of the sample with 10% wt is lower than 70% because of the excess filler. It is obviously observed that the physical water plasticization makes the retention rate of impact strength over 150% in all samples. For those samples filled with various contents of sepiolite, the rates are higher than that of PA6/LGF sample, especially for the sample with 8%wt Sep, a nearly 200% retention rate is observed clearly. These results from the retention rate of mechanical properties above indicates that certain content (6-8%) of sepiolite in PA6/LGF/Sep composites can keep tensile strength at a stable level and increase the retention rate of impact strength in long time ageing, which is positive for the composites to serve in hygrothermal environment. By the way, the samples filled with 10%wt sepiolites show a worse retention rate of mechanical properties because an excessive addition of filler (sepiolites) can cause a

severe deterioration in mechanical properties.

In value of number, PA6/LGF/Sep shows a global decreasing trend both in tensile and impact strength with the addition of sepiolite. We infer that the mechanical properties of the composites are mainly relying on the LGF. It can also be indicated that the sepiolite has some rejected effects with glass fibre on the reinforcing polymer composites. Fortunately, because of the existence of enough (30%wt) LGF, the mechanical properties of the composites are still staying at a relatively high level for application in many areas. What's more, for all the different content of sepiolite, the samples with 8% wt sepiolite have the most stable tensile and impact strength and the highest retention rate of impact strength in the hygrothermal ageing period from 5 to 20d. For those samples, the variations of the tensile and impact strength were less than 3.1% and 5.5%, respectively. By the way, when the content of seipolite reaches 10%, it will be difficult to extrude the mastbatches. So the content of 8% wt of sepiolite will be typical to be the stabilizer of PA6/LGF composites analyzed below.

### *3.2 Fracture morphology*

The SEM images were applied to analyze the interface between LGF and PA6 matrix in long time hygrothermal ageing. There are three ways of the energy absorption of fibre reinforced composites deformation: the breakage of glass fibre, fibre pulling out and matrix rupture [14]. When stress acts on composites, internal shear stress will transfer the external stress from matrix to fibres [15]. The impact section morphologies of PA6/LGF composites are shown in Fig. 5. For unaged ones in Fig. 5 (A and C), the samples with sepiolite show the same fracture morphology which both include the breakage and pulling out of glass fibre. For sample aged for 20 d in Fig. 5(B), it can be observed that several smooth glass fibres without coating are pulled out which means the interface debond severely after long time hygrothermal



ageing. While in the sample filled with 8% sepiolite (Fig. 5D), glass fibres pulled out have a relatively rough surface with adhesive interface attributed to the water absorption of sepiolite, which can protect the matrix and interface from the debonding of water molecule erosion. The effects of temperature and water molecules in hygrothermal environment on polymer-fibre composites are mainly on the interface between fibre and polymer matrix. In this course, the interface failure causes the decrease of tensile and impact strength while the increase of impact strength is caused by water plasticization of PA6 matrix. Samples filled with certain contents of sepiolites show better interface properties as exhibited above. The better interface properties, the higher retention rate of tensile and impact strength.

### 3.3 Thermal stability

The TGA has been widely used to investigate the thermal properties of polymer composites. We defined  $T_{5\%}$  as the onset decomposition temperature of composites which means 5% weight loss, and  $T_{\max}$  as the peak temperature of DTG which means the highest weight loss rate. The TGA curves of PA6/LGF/Sep with different content of sepiolite at a heating rate of 10 °C/min are shown in Fig. 6. In this work, the PA6/LGF composites with and without sepiolite both show only one decomposition process. With the addition of sepiolite, the TGA curves move slightly to a low temperature. And  $T_{5\%}$  increases from 353.4°C to 361.8°C while  $T_{\max}$  decreases from 458.9°C to 445.8°C (details in Table 1), which means the sepiolite makes the thermal decomposition temperature range narrower in PA6/LGF/Sep composites. At the same time, it is clearly seen that the content of degradation residue increases with increasing the content sepiolite. Degradation residues can form carbon layers which can be stable at high temperature on the surface of materials, and the layers can isolate air, volatile combust and heat flow from polymer matrix to protect the composites.

The TGA of PA6/LGF and PA6/LGF/Sep composites with different hygrothermal ageing time at the same heating rate of 10°C/min are exhibited in Fig. 7. From 0 day to 15 days ageing, there are very slight variations in TGA curves for PA6/LGF composites, however, the ageing time reaches 20d, an obvious decrease in  $T_{\max}$ , which means a serious decrease in thermal stability. It is due to the chain breakage of PA6 molecule after the hygrothermal ageing which include not only interface debonding but also matrix degradation caused by water corrosion. With enough ageing time, degraded PA6 with shorter molecular chain has a worse thermal stability. Furthermore, it can be observed that the degradation residues have a slight decrease with enough long time ageing (15 and 20d).

For the PA6/LGF/Sep composites, it can be found from Fig. 7 B that TGA curves move to higher temperature with longer ageing time, which means an increase in thermal stability. It is very interesting that the residues of each sample has a different degree of variation, it is also attributed to the migration of sepiolite from inner structure to sample surface even out of samples in different period of hygrothermal ageing. A small amount of sepiolite which absorbed water flow out from samples as narrated above which can cause a slight change of sample weight. Because of this course, it is difficult to explain the changes only with TGA data at one constant heating rate. Then the variation of thermal stability can be analyzed by kinetic methods thereafter in details.

### 3.4 Thermal degradation kinetics

The application of dynamic TGA methods holds good promise as a tool for unraveling the mechanisms of physical and chemical processes that occur during degradation of a polymer and its composites [16]. The curves and detail TGA data of the unaged and aged 20d composites, including  $T_{5\%}$  (temperature of 5% weight loss),

$T_{\max}$  (temperature of maximum decomposition rate),  $d\alpha/dT$  (the maximum weight losing rate), under a heat flow of nitrogen at a heating rate of from 10 to 40 °C/min are listed in Fig. 8, Tables 1 and 2. To analyze the effect of long time hygrothermal ageing on degradation kinetic properties of PA6/LGF/Sep composites, the apparent active energy ( $E$ ) values of the unaged and aged composites are calculated by three methods (including Kissinger, Friedman and Flynn-Wall-Ozawa method).

In the kinetic studies of this work, we first assume that the isothermal rate of conversion,  $d\alpha/dT$ , is a linear function of the reactant concentration loss and of the temperature-independent rate constant,  $k$ , and a temperature independent function of conversion, it can be represented by the equation of:

$$d\alpha/dt = \beta (d\alpha/dT) = k(T)f(\alpha) = k(1-\alpha)^n \quad (1)$$

where  $f(\alpha)$  and  $k(T)$  are the functions of conversion and temperature,  $\alpha$  the degree of conversion,  $\beta$  the heating rate ( $\beta = dT/dt$ ),  $k$  the rate constant,  $n$  the apparent order of reaction. The temperature dependence of the kinetic constant ( $k$ ) is given by the Arrhenius equation:

$$k = A \exp(-E/RT) \quad (2)$$

In which  $E$  is the activation energy of the reaction,  $A$  is the frequency factor,  $T$  is the reaction temperature, and  $R$  is the gas constant. Combination of equations (1) and (2) gives the following equation:

$$d\alpha/dT = A(1-\alpha)^n \exp(-E/RT) \quad (3)$$

which occurs to the following relationship of the basis of many analytical approaches to calculate the kinetic parameters. Equation (3) is normally the fundamental base for the kinetic analysis of a solid material from nonisothermal TGA data.

Kissinger method [17] thinks that apparent order of reaction ( $n$ ) can be ignored when temperature reaches the maximum weight losing temperature ( $T_{\max}$ ). It shows

that  $T_{\max}$  can be used to calculate the apparent Arrhenius activation energy by this equation:

$$\ln(\beta/T_{\max}) = \ln(AR/E) - E/RT_{\max} \quad (4)$$

where  $\beta$ ,  $T_{\max}$  and  $R$  are heating rate, the peak absolute temperature, and the gas constant, respectively. With this method, we obtain the values of activation energy ( $E$ ) from the slope of straight line plot of  $\ln(\beta/T_{\max})$  versus  $1/T_{\max}$ .

On the other hand, Friedman [18] gives the following equation:

$$\ln(\beta d\alpha/dT) = \ln[Af(\alpha)] - E/RT \quad (5)$$

by calculating the natural logarithm on the both sides of equation (3). The value of  $d\alpha/dT$  can approximate the weight losing rate which can be obtained from DTG data. If we can acquire the data of weight losing rate at a certain temperature, the values of  $E$  should be obtained from the slope of the straight line plot of  $\ln(\beta d\alpha/dT)$  versus  $1/T$ . In this work, the  $T_{\max}$  is also chosen in Friedman method.

The analysis of Kissinger and Friedman method are exhibited in Fig. 9, which shows the plots of  $\ln(\beta/T_{\max})$  and  $\ln(\beta d\alpha/dT)$  versus  $1/T$  at varying conversion, respectively. Application of the analytical technique to the data presented in Table 1 and Table 2 gives the mean values of activation energy calculated from the 4 different heating rates which are summarized in Table 3. For PA6/LGF 20d aged samples,  $T_{\max}$  of the heating rate of 40 °C/min is much lower than that of 30 °C/min. This may be attributed to the diffusion of water molecule in PA6 molecular chain which leads to a partial hydrolyzation after long time hygrothermal ageing. So only the heating rates of 10–30 °C/min were used to calculate the value of  $E$  in this sample.

From the  $E$  results, for PA6/LGF samples without sepiolite, it is obviously seen that the value of  $E$  has a serious decrease of 35.8% and 58.4% by Kissinger and Friedman methods with longer ageing time, respectively. This indicates that the

hygrothermal ageing results in a sharp decline in the thermal stability of the composites, which can also be attributed to the hydrolyzation of PA6 molecular chain. Those samples filled with sepiolites show a relatively steady value of  $E$  with longer ageing time of which variations are 7.5% increase and 4.8% decrease by Kissinger and Friedman methods, respectively.

The above technique of Kissinger and Friedman has some merit in providing kinetic data, but it is defective that only use one data point (at  $T_{\max}$ ) for the whole degradation stage. Another kinetic method used in this work is Flynn-Wall-Ozawa method [19, 20], which is probably the most general derivative method [21]. This method uses an integral solution and it is also independent of the degradation mechanism. Then from Doyle approximation, we can get the following equation:

$$\lg \beta = \lg [AE/RG(\alpha)] - 2.315 - 0.4567E/RT \quad (6)$$

In this work, we use conversion values in the range of 20–60% with this method. The plot of  $\log \beta$  against  $1/T$  at a fixed degree of conversion  $\alpha$  should give a straight whose slope is proportional to  $E$ , including the temperature with different partial mass loss rate of 0.2, 0.3, 0.4, 0.5, and 0.6. The analysis of Flynn-Wall-Ozawa is shown in Fig. 10, and the  $E$  values corresponding to different conversions are given in Fig. 11.

Fig. 11 reveals that unaged PA6/LGF shows a steady level of  $E$  at  $\alpha$  value of 0.2–0.6. Then after 20d hygrothermal ageing, an obvious decrease of 27.8% of  $E$  can be observed as same as the results calculated by the other two methods. What's more, a decrease of  $E$  with the partial mass loss increasing occurs, which means the aged samples appear to have a lower  $E$  in the later stages of the degradation. It is indicated that aged PA6/LGF is in a lower and lower energy barrier state of thermal kinetics with the progress of thermal degradation. On the contrary, the PA6/LGF/Sep filled with 8% wt sepiolites display only a slightly increase of  $E$  after ageing as the same

trend of the results calculated by Kissinger method. With the addition of sepiolites, a much more steady thermal kinetics state of the samples has been achieved.

Then the  $E$  values calculated by all the three methods are listed in Table 4. It is clearly observed that the  $E$  values of the unaged and aged composites filled with 8%wt sepiolite are higher than that without sepiolite calculated by the three methods. It means that the sepiolites can improve the thermal stability of PA6/LGF, which can be used to enhance the flame retardancy of the composites. Then for 20d aged ones,  $E$  values of samples without sepiolite have a varying degrees of decline calculated by the three methods while the composites filled with sepiolite show a slightly increase of 6.9% and 7.3% by Kissinger and Flynn-Wall-Ozawa method, respectively.

Through analyzing the  $E$  obtained from the Kissinger, Friedman and Flynn-Wall-Ozawa methods, it is found that the effect of long time hygrothermal ageing on the  $E$  of the composites filled with sepiolites is much lesser than that of the composites without it. It can be attributed to the water absorption of sepiolite which reduces the water diffusion into PA6 matrix and protects PA6 and glass fibre from water corrosion including the PA6 molecular chain hydrolyzation and interface debonding. The presence of sepiolite makes PA6/LGF composites have a better thermal stability to stay at a relatively steady state in both thermodynamics and kinetics against hygrothermal environment.

#### 4. Conclusions

This exploratory work investigates the effect of hygrothermal ageing on the mechanical properties and thermal degradation kinetics of PA6/LGF composites filled with sepiolite. With the addition of different contents of sepiolite into PA6/LGF, the mechanical properties of the composites have a decrease, but still stay at a high level for application because of the presence of enough glass fibre. With long time

hygrothermal ageing, the tensile strength of the composites decreases, however, the impact strength increases, which means a plastification trend caused by the water absorption of PA6 matrix and the plastification trend can be slighter for PA6/LGF/Sep composites. Then the impact fracture morphology indicates that an obvious interface debonding occurs in the samples without sepiolite. The thermal stability and kinetic analysis show that the apparent  $E$  values of PA6/LGF calculated by Kissinger, Friedman and Flynn-Wall-Ozawa methods have a sharp decrease with long time hygrothermal ageing, which can be attributed to the PA6 molecular chain hydrolyzation, however, the value of  $E$  of composites filled with sepiolites has only a slight increase. In conclusion, sepiolite can work as a relatively nice filler in the PA6/LGF composites against the hygrothermal environment. The composites filled with sepiolites have a higher value of  $E$  which means better thermal stability, and it is also feasible to use sepiolite in the application of flame retardant system.

### Acknowledgments

The authors are grateful to the high level innovation talents cultivation of Guizhou Province ([2015]4039), National Natural Science Foundation of China (51003088), Opening Project of State Key Laboratory of Polymer Materials Engineering (Sichuan University) (sklpme2014-4-21), and Fundamental Research Funds for the Central Universities (SWJTU12CX009) for financial support of this work.

## References

1. W. Yan, K. Han, L. Qin, M. Yu. *J Appl Polym Sci.* 2004; 91: 3959–3965.
2. X. Zuo, H. Shao, D. Zhang, Z. Hao, J. Guo. *Polym Deg & Stab.* 2013; 98: 2774-2783.
3. G. Carra, V. Carvelli. *Comp Struct.* 2014; 108: 1019–1026.
4. M. Foulc, A. Bergeret, L. Ferry, P. Ienny. *Polym Deg & Stab.* 2005; 89: 461–470.
5. M. Akay. *Polym Comp.* 1994; 2: 349–354.
6. A. Nohales, L. Solar, I. Porcar, C. Vallo, C. Gomez. *Eur Polym J.* 2006; 42: 3093-3101.
7. J. Ma, E. Bilotti, T. Peijs, J. Darr. *Eur Polym J.* 2007; 43: 4931–4939.
8. H. Bidsorkhi, M. Soheilmoghaddam, R. Pour, H. Adelnia, Z. Mohamad. *Polym Test.* 2014; 37: 117–122;
9. W. Kuang, G. Facey, C. Detellier, B. Casal, J. Serratosa, E. Ruiz-Hitzky. *Chem Mater.* 2003; 15: 4956–4967.
10. W. Kuang, G. Facey, C. Detellier. *Chem Mater.* 2006; 26: 179–185.
11. S. Li, X. Hu, Y. Wang, C. Xie. *Acta Mater Compo Sin.* 2012; 29: 73–78.
12. Y. Turhan, P. Turan, M. Dogan, M. Alkan, H. Namli, O. Demirbas. *Ind & Eng Chem Res.* 2008; 47: 1883–1895.
13. M. Alkan, G. Tekin, H. Namil. *Micropo & Mesopo Mater.* 2005; 84: 75–83.
14. K. Han, Z. Liu, M. Yu. *Macromo Mater Eng.* 2005; 290: 688–694.
15. M. Kennedy, E. Cuellar, D. Roberts. *Fibre Optic Components & Reliability.* 1992; 1: 152–162.
16. X. Chen, J. Yu, S. Guo. *J Appl Polym Sci.* 2007; 103: 1978–1984.
17. H. Kissinger. *Anal Chem.* 1957; 29: 1702–1706.
18. H. Friedman. *J Macromo Sci, A Chem.* 1967; 41: 57–79.
19. T. Ozawa. *Bull chem soc Jap.* 1965; 38: 1881–1886.



20. J. Flynn, L. Wall. *Polym Lett.* 1966; 4; 323–328.
21. X. Chen, J. Yu, Z. Luo, S. Hu, Z. Zhou, S. Guo. *J Polym Res.* 2009; 16: 745–753.

### The Captions of Figures

Fig. 1. Variations of tensile strength with ageing time for PA6/LGF/Sep composites.

Fig. 2. Variations of impact strength with ageing time for PA6/LGF/Sep composites.

Fig. 3. The retention rate of tensile strength with ageing time for PA6/LGF/Sep composites.

Fig. 4. The retention rate of impact strength with ageing time for PA6/LGF/Sep composites.

Fig. 5. The SEM images of the impact section morphology with 500X magnification: (A) PA6/LGF, unaged; (B) PA6/LGF, 20 d aged; (C) PA6/LGF/Sep 8%, unaged; (D) PA6/LGF/Sep 8%, 20 d aged.

Fig. 6. TGA curves of PA6/LGF/Sep composites with different amount of sepiolite.

Fig. 7. TGA curves of (A) PA6/LGF and (B) PA6/LGF/Sep with different ageing time.

Fig. 8. The TGA curves with different heating rates of 10, 20, 30, and 40°C/min for (A) PA6/LGF, unaged; (B) PA6/LGF, 20d aged; (C) PA6/LGF/8%Sep, unaged; (D) PA6/LGF/8%Sep, 20d aged.

Fig. 9. Plots of  $\ln(\beta/T_{\max}^2)$  and  $\ln(\beta d\alpha/dT)$  versus  $1/T_{\max}$  at different heating rates according to Kissinger and Friedman methods: (A) PA6/LGF, unaged; (B) PA6/LGF, 20d aged; (C) PA6/LGF/8%Sep, unaged; (D) PA6/LGF/8%Sep, 20d aged.

Fig. 10. The  $\lg\beta-1/T$  curves with different partial mass loss of (A) PA6/LGF, unaged; (B) PA6/LGF, 20d aged; (C) PA6/LGF/8%Sep, unaged; (D) PA6/LGF/8%Sep, 20d aged.

Fig. 11. The activation energy ( $E$ ) of unaged and 20 d aged samples with partial mass loss by Flynn-Wall-Ozawa method.

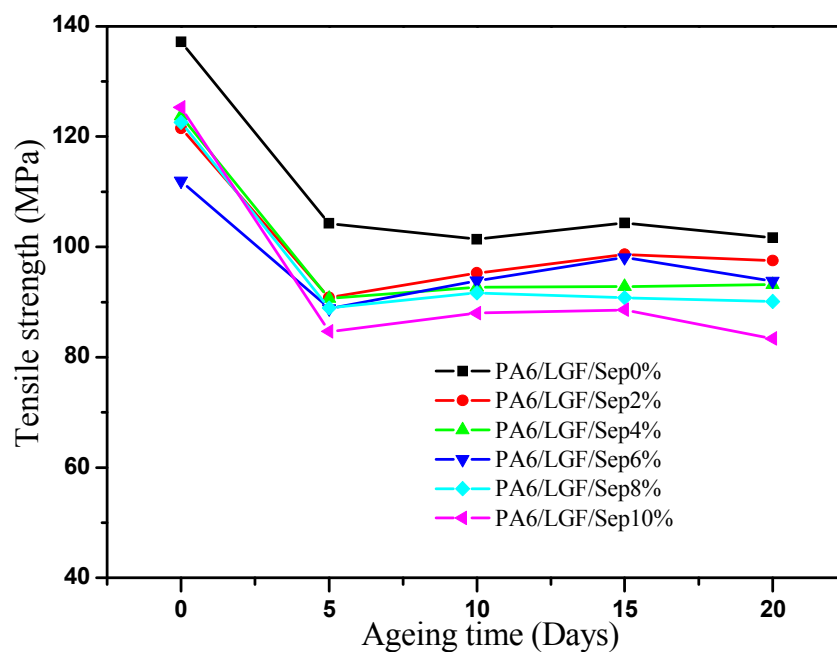


Fig. 1. Variations of tensile strength with ageing time for PA6/LGF/Sep composites

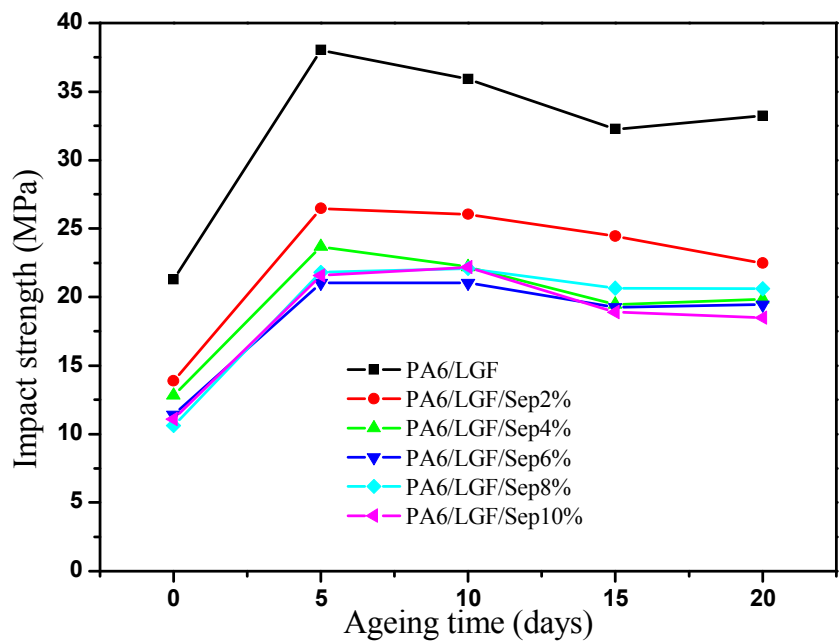


Fig. 2. Variations of impact strength with ageing time for PA6/LGF/Sep composites

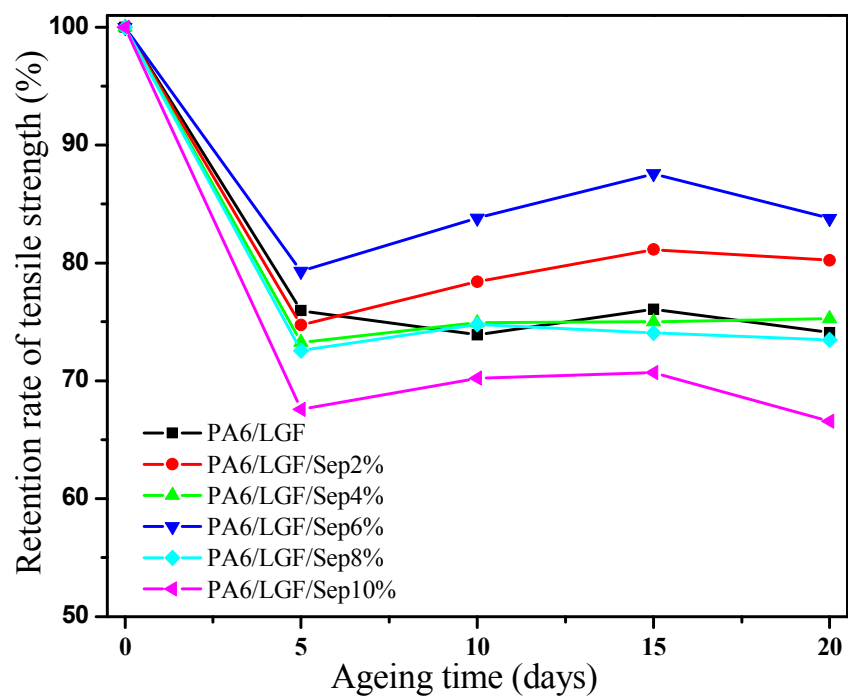


Fig. 3. The retention rate of tensile strength with ageing time for PA6/LGF/Sep composites

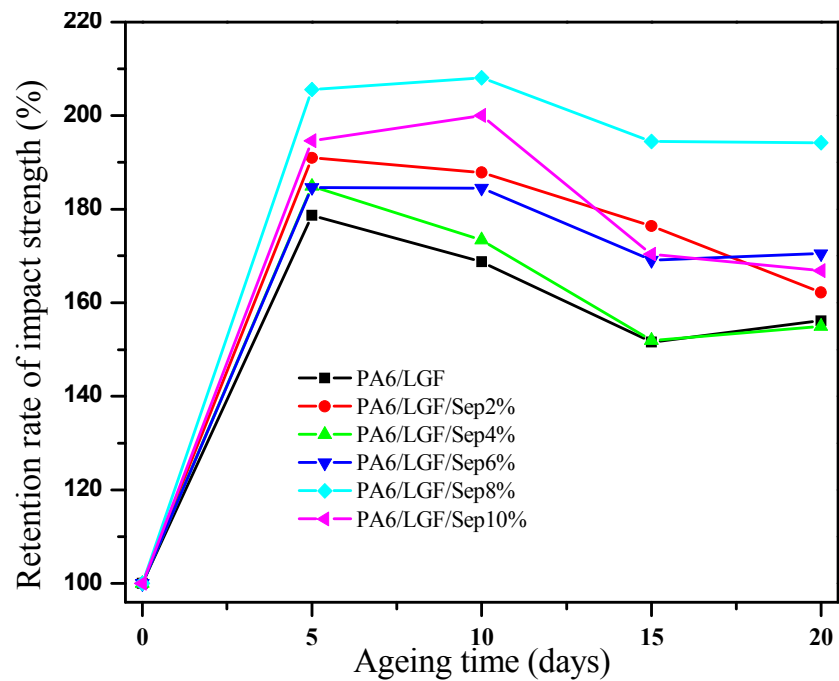


Fig. 4. The retention rate of impact strength with ageing time for PA6/LGF/Sep composites

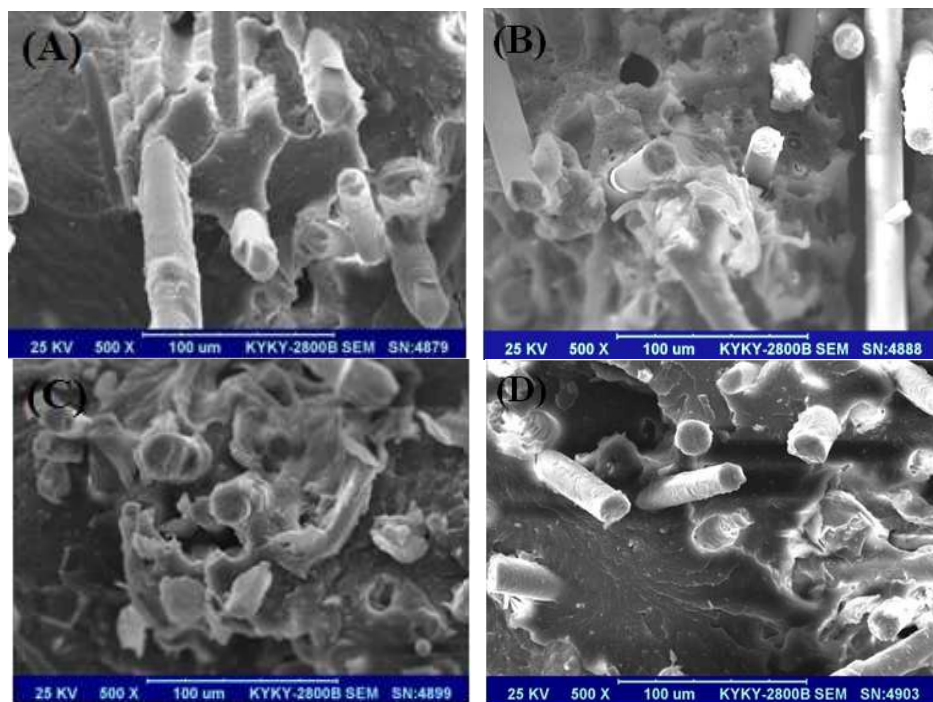


Fig. 5. The SEM images of the impact section morphology with 500X magnification: (A) PA6/LGF, unaged; (B) PA6/LGF, 20 d aged; (C) PA6/LGF/Sep 8%, unaged; (D) PA6/LGF/Sep 8%, 20 d aged.

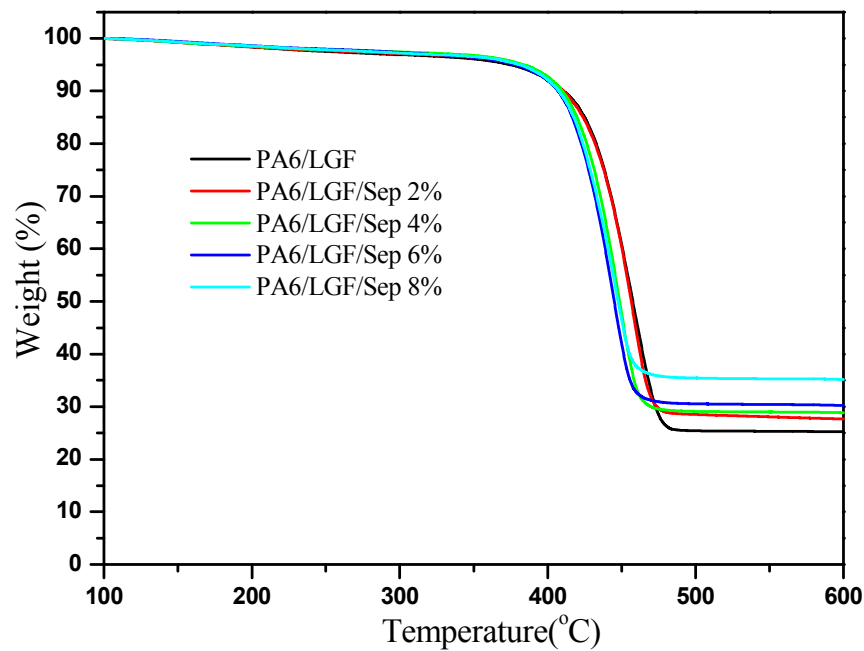


Fig. 6. TGA curves of PA6/LGF/Sep composites with different amount of sepiolite.



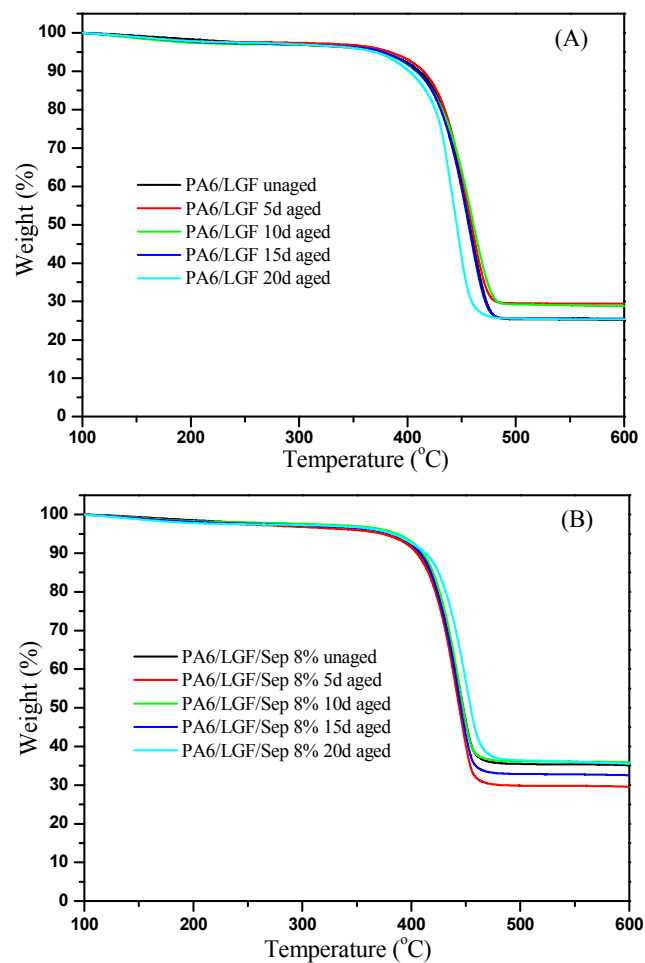


Fig. 7. TGA curves of (A) PA6/LGF and (B) PA6/LGF/Sep with different ageing time.

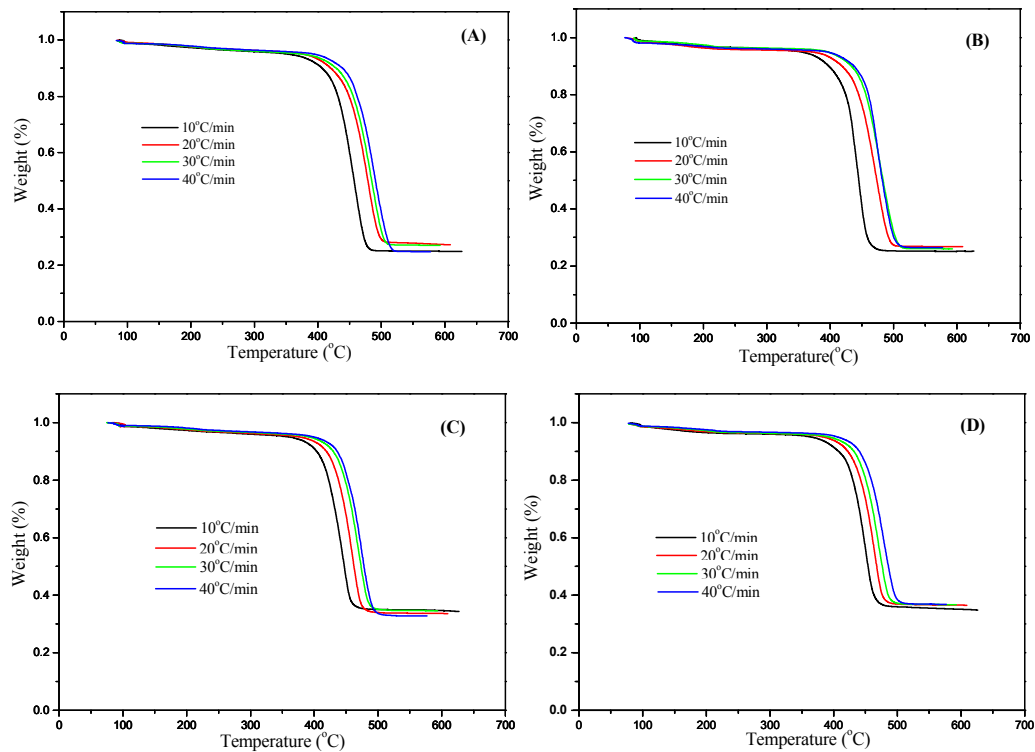


Fig. 8. The TGA curves with different heating rates of 10, 20, 30, and 40°C/min for (A) PA6/LGF, unaged; (B) PA6/LGF, 20d aged; (C) PA6/LGF/8%Sep, unaged; (D) PA6/LGF/8%Sep, 20d aged.

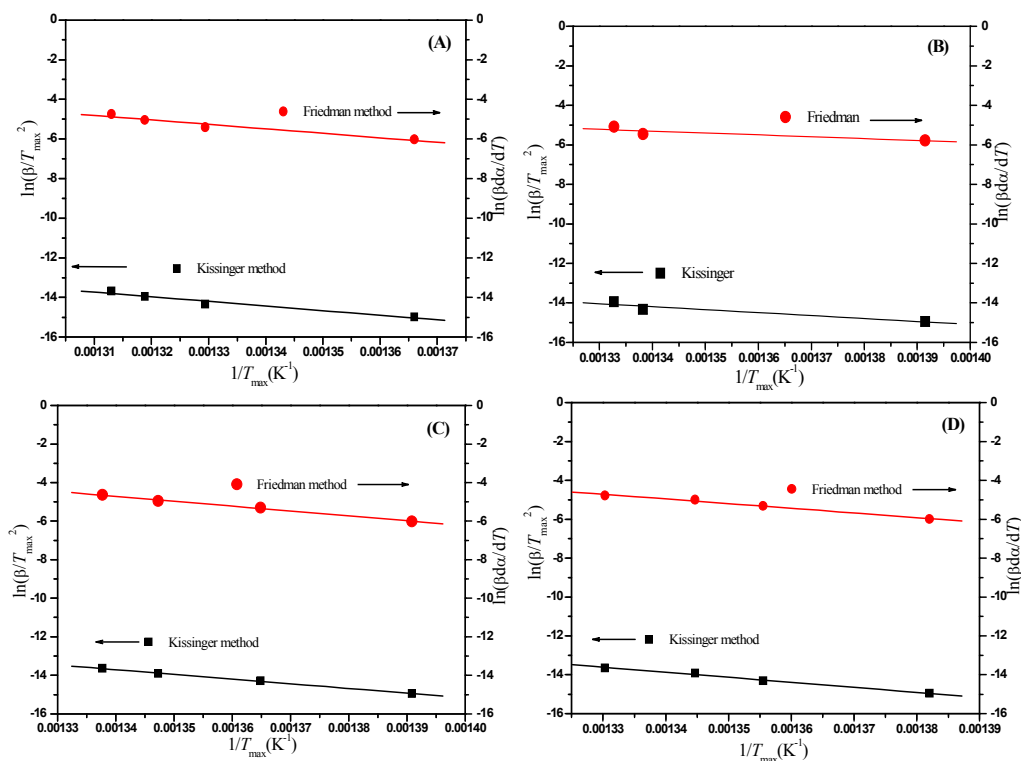


Fig. 9. Plots of  $\ln(\beta/T_{\max}^2)$  and  $\ln(\beta d\alpha/dT)$  versus  $1/T_{\max}$  at different heating rates according to Kissinger and Friedman methods: (A) PA6/LGF, unaged; (B) PA6/LGF, 20d aged; (C) PA6/LGF/8%Sep, unaged; (D) PA6/LGF/8%Sep, 20d aged.

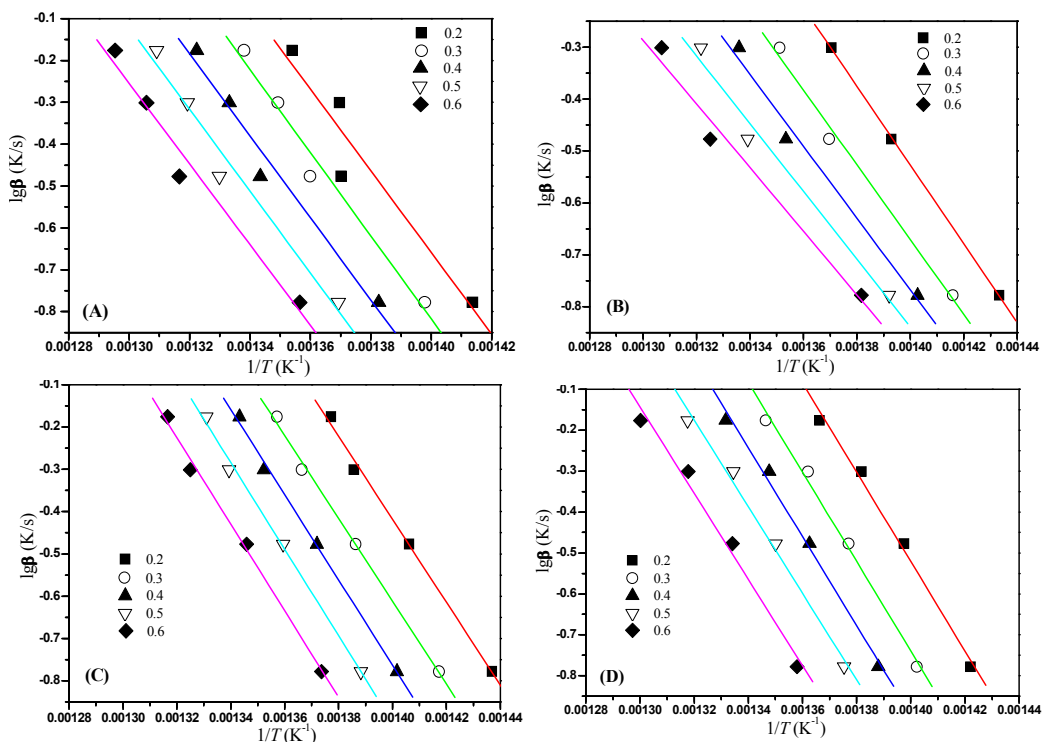


Fig. 10. The  $\lg\beta$ - $1/T$  curves with different partial mass loss of (A) PA6/LGF, unaged; (B) PA6/LGF, 20d aged; (C) PA6/LGF/8%Sep, unaged; (D) PA6/LGF/8%Sep, 20d aged.

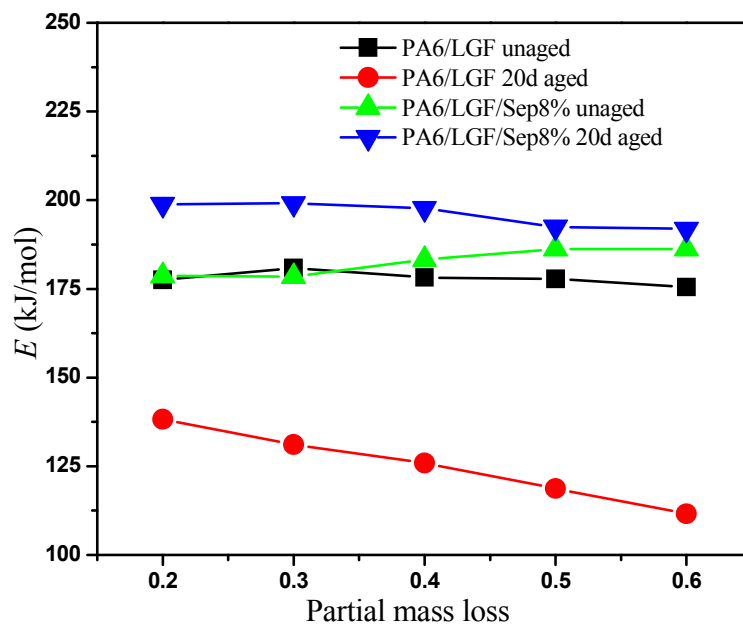


Fig. 11. The activation energy ( $E$ ) of unaged and 20 d aged samples with partial mass loss by Flynn-Wall-Ozawa method.

Table 1 The TGA data of unaged and aged PA6/LGF/Sep composites

Temperature characteristic point	$T_{5\%}(^{\circ}\text{C})$				$T_{\text{max}}(^{\circ}\text{C})$			
	Sep0% 0d	Sep0% 20d	Sep8% 0d	Sep8% 20d	Sep0% 0d	Sep0% 20d	Sep8% 0d	Sep8% 20d
10°C/min	353.4	354.1	361.8	358.8	458.9	445.50	445.8	450.4
20°C/min	377.5	354.0	378.0	381.5	479.1	474.10	459.5	464.6
30°C/min	375.1	396.1	392.7	390.6	485.1	477.17	469.1	470.5
40°C/min	394.6	394.4	399.9	399.3	488.5	474.06	474.4	478.6

Table 2 Weight losing rate of unaged and aged PA6/LGF/Sep from the TGA analysis.

Temperature characteristic point	$da/dT (\%/^{\circ}\text{C})$			
	Sep 0%, 0d	Sep 0%, 20d	Sep 8%, 0d	Sep 8%, 20d
10 °C/min	1.445	1.865	1.464	1.503
20 °C/min	1.350	1.278	1.496	1.463
30 °C/min	1.288	1.244	1.407	1.359
40 °C/min	1.309	1.562	1.460	1.264

Table 3 Activation energy of PA6/LGF/Sep composites obtained by Kissinger and Friedman method.

Samples	PA6/LGF 0d	PA6/LGF 20d	PA6/LGF/Sep 0d	PA6/LGF/Sep20d
Kissinger $E$ (kJ/mol)	193.41	124.25	201.77	215.68
Correlation coefficient	0.9537	0.9037	0.9963	0.9922
Friedman $E$ (kJ/mol)	188.59	78.45	210.53	200.43
Correlation coefficient	0.9500	0.7771	0.9943	0.9890

Table 4. Comparison of activation energy of PA6/LGF/Sep composites obtained by three methods

Samples	Kissinger $E$ (kJ/mol)	Friedman $E$ (kJ/mol)	F-W-O $E$ (kJ/mol)
PA6/LGF 0d	178.130	188.586	177.845
PA6/LGF 20d	124.252	78.451	128.481
PA6/LGF/Sep 0d	201.772	210.527	182.608
PA6/LGF/Sep 20d	215.681	200.433	196.012